

Submicron Streptavidin Patterns for Protein Assembly

Karen L. Christman,^{†,‡} Michael V. Requa,[§] Vanessa D. Enriquez-Rios,[†] Sabrina C. Ward,^{||}
Kenneth A. Bradley,^{||,‡} Kimberly L. Turner,^{§,‡} and Heather D. Maynard^{*,†,‡}

Department of Chemistry and Biochemistry, Department of Microbiology, Immunology, and Molecular Genetics, California NanoSystems Institute, University of California, Los Angeles, Los Angeles, California, 90095, and Department of Mechanical Engineering, California NanoSystems Institute, University of California, Santa Barbara, Santa Barbara, California 93106

Received March 28, 2006. In Final Form: May 26, 2006

Micron and submicron-scale features of aldehyde functionality were fabricated in polymer films by photolithography to develop a platform for protein immobilization and assembly at a biologically relevant scale. Films containing the pH-reactive polymer poly(3,3'-diethoxypropyl methacrylate) and a photoacid generator (PAG) were patterned from 500 nm to 40 μm by exposure to 365 nm (i-line) light. Upon PAG activation and hydrolysis of acetals, aldehyde groups formed. After the films were incubated with a biotinylated aldehyde reactive probe, the X-ray photoelectron spectroscopy results were consistent with biotin being attached to the surface. The background was subsequently passivated by flood exposure and incubation with an aminoxy-terminated poly(ethylene glycol), resulting in a 98% reduction in nonspecific protein adsorption. Protein patterning and assembly was demonstrated using streptavidin, biotinylated anthrax toxin receptor-1, and the protective antigen moiety of anthrax toxin and confirmed by fluorescence microscopy and atomic force microscopy (AFM). AFM demonstrated that 500 nm protein features were achieved. Because of the abundance of biotinylated proteins, this methodology provides a platform for protein immobilization and assembly for various applications in biotechnology.

Introduction

Routes to site-specifically immobilize proteins and form protein assemblies at the submicron and nanometer scale have importance in a variety of applications including nanodevices, implant coatings, and tissue engineering.¹ Several methods have been explored to pattern proteins smaller than 1 μm .² Scanning probe lithographic techniques, such as nanografting^{3–7} and dip-pen nanolithography (DPN),^{8–15} are the most commonly investigated.

For example, carboxylic acid^{3,4} and aldehyde-terminated³ patterns have been grafted into methyl-terminated self-assembled monolayers (SAMs). Proteins were adsorbed onto the carboxylic acids or chemically coupled using 1-ethyl-3-(3-dimethylaminopropyl) carbodiimide hydrochloride (EDC) chemistry.⁴ Proteins were attached to aldehydes through free amines, forming imine bonds.³ To create a more protein resistant background, tri(ethylene glycol)-terminated SAMs have also been utilized.⁴ Furthermore, metalloproteins containing C-terminal thiol groups have been directly grafted into octadecanethiol SAMs.⁵ The majority of studies using indirect DPN have deposited 16-mercaptohexadecanoic acid for subsequent protein adsorption^{8,9,16} or attachment of amine-terminated biotin after activation of the acids with *N*-hydroxysuccinimide (NHS) and EDC.¹⁰ The deposition of NHS-biotin on polyethylenimine surfaces for streptavidin immobilization¹¹ and on a maleimide-terminated disulfide for protein attachment via free cysteines¹⁷ has also been explored. Thiolated proteins have been delivered onto gold substrates,¹² while histidine-tagged proteins have been deposited onto nickel substrates¹⁸ using direct DPN methods. Proteins have also been patterned onto glycidoxypolytrimethoxysilane-coated glass¹³ and aldehyde-modified surfaces.¹⁵ High resolutions are achieved with such methods; however, they are serial techniques that are limited by speed and inhibit patterning over large areas.

Stamp-based methods such as nanocontact printing^{19–21} and nanoimprint lithography^{22,23} have also been employed for

* Corresponding author. E-mail: maynard@chem.ucla.edu. Phone: (310) 267-5162. Address: Department of Chemistry and Biochemistry, 607 Charles E. Young Drive East, University of California, Los Angeles, CA 90095-1569.

[†] Department of Chemistry and Biochemistry, University of California, Los Angeles.

[‡] California NanoSystems Institute, University of California, Los Angeles, Santa Barbara.

[§] Department of Mechanical Engineering, University of California, Santa Barbara.

^{||} Department of Microbiology, Immunology, and Molecular Genetics, University of California, Los Angeles.

(1) Astier, Y.; Bayley, H.; Howorka, S. *Curr. Opin. Chem. Biol.* **2005**, *9*, 576–584.

(2) Voros, J.; Blattler, T.; Textor, M. *MRS Bull.* **2005**, *30*, 202–206.

(3) Wadu-Mesthrige, K.; Xu, S.; Amro, N. A.; Liu, G. Y. *Langmuir* **1999**, *15*, 8580–8583.

(4) Kenseth, J. R.; Harnisch, J. A.; Jones, V. W.; Porter, M. D. *Langmuir* **2001**, *17*, 4105–4112.

(5) Case, M. A.; McLendon, G. L.; Hu, Y.; Vanderlick, T. K.; Scoles, G. *Nano Lett.* **2003**, *3*, 425–429.

(6) Zhou, D. J.; Wang, X. Z.; Birch, L.; Rayment, T.; Abell, C. *Langmuir* **2003**, *19*, 10557–10562.

(7) Nuraje, N.; Banerjee, I. A.; MacCuspie, R. I.; Yu, L. T.; Matsui, H. *J. Am. Chem. Soc.* **2004**, *126*, 8088–8089.

(8) Lee, K. B.; Park, S. J.; Mirkin, C. A.; Smith, J. C.; Mrksich, M. *Science* **2002**, *295*, 1702–1705.

(9) Kwak, S. K.; Lee, G. S.; Ahn, D. J.; Choi, J. W. *Mater. Sci. Eng., C* **2004**, *24*, 151–155.

(10) Hyun, J.; Ahn, S. J.; Lee, W. K.; Chilkoti, A.; Zauscher, S. *Nano Lett.* **2002**, *2*, 1203–1207.

(11) Pena, D. J.; Raphael, M. P.; Byers, J. M. *Langmuir* **2003**, *19*, 9028–9032.

(12) Wilson, D. L.; Martin, R.; Hong, S.; Cronin-Golomb, M.; Mirkin, C. A.; Kaplan, D. L. *Proc. Natl. Acad. Sci. U.S.A.* **2001**, *98*, 13660–13664.

(13) Noy, A.; Miller, A. E.; Klare, J. E.; Weeks, B. L.; Woods, B. W.; DeYoreo, J. J. *Nano Lett.* **2002**, *2*, 109–112.

(14) Agarwal, G.; Sowards, L. A.; Naik, R. R.; Stone, M. O. *J. Am. Chem. Soc.* **2003**, *125*, 580–583.

(15) Lim, J. H.; Ginger, D. S.; Lee, K. B.; Heo, J.; Nam, J. M.; Mirkin, C. A. *Angew. Chem., Int. Ed.* **2003**, *42*, 2309–2312.

(16) Lee, K. B.; Kim, E. Y.; Mirkin, C. A.; Wolinsky, S. M. *Nano Lett.* **2004**, *4*, 1869–1872.

(17) Smith, J. C.; Lee, K. B.; Wang, Q.; Finn, M. G.; Johnson, J. E.; Mrksich, M.; Mirkin, C. A. *Nano Lett.* **2003**, *3*, 883–886.

(18) Nam, J. M.; Han, S. W.; Lee, K. B.; Liu, X. G.; Ratner, M. A.; Mirkin, C. A. *Angew. Chem., Int. Ed.* **2004**, *43*, 1246–1249.

(19) Renault, J. P.; Bernard, A.; Bietsch, A.; Michel, B.; Bosshard, H. R.; Delamarche, E.; Kreiter, M.; Hecht, B.; Wild, U. P. *J. Phys. Chem. B* **2003**, *107*, 703–711.

immobilizing proteins with submicron resolution. Nanocontact printing is essentially the same technique as microcontact printing, which was first developed by Whitesides and co-workers,^{24,25} but generates patterns with higher resolution. Patterns have been reduced to the nanoscale with nanocontact printing by decreasing the feature sizes in the poly(dimethylsiloxane) (PDMS) stamp and diluting the protein inks,¹⁹ utilizing an atomic force microscopy (AFM) V-shaped test grating as the master for hard PDMS stamps,²⁰ or employing polyolefin stamps.²¹ Nanoimprint lithography also makes use of a stamp; however, the stamp is used to create topographical features in the substrate, which can then be modified for the immobilization of proteins. This technique has been employed to create SiO₂ patterns that are then coated with an amine-terminated silane for functionalization with biotin-succinimidyl ester, followed by streptavidin.²² Nb₂O₅ patterns have also been generated for the immobilization of biotin functionalized poly(L-lysine)-g-poly(ethylene glycol).²³ While the resolution of AFM-based methods cannot yet be matched with such stamp-based techniques, patterns over large areas ranging from hundreds or thousands of microns can be achieved.

Many studies have demonstrated the utility of photochemical lithography for patterning at the micron scale. Micropatterns of amine-terminated monolayers have been fabricated by deprotection with ultraviolet (UV) radiation.^{26–28} Anti-biotin antibody patterns were created in one study after linking biotin to the amines.²⁸ Other studies have employed UV radiation to convert the end-groups of monolayers^{29–31} as well as polymers in the presence of a photoacid generator³² to COOH derivatives. Thiol-terminated silane monolayers have also been patterned by UV-induced oxidation.^{33–35} We recently reported the fabrication of a pH-responsive polymer film that was chemically transformed using photolithography to produce 18 × 18 micron-sized protein patterns.³⁶ The spin-coated film consisted of poly(3,3'-diethoxypropyl methacrylate) (PDEPMA) with acetal side chains that were hydrolyzed to aldehydes upon exposure to deep UV radiation in the presence of a photoacid generator (PAG). Aldehydes react under mild aqueous conditions,³⁷ and are therefore an excellent functionality for immobilizing biomolecules on surfaces. For example, aminoxy-modified molecules conjugate to aldehydes without the addition of any other reagent. This could allow for the specific immobilization of peptides and proteins, rather than adsorption to patterned proteinophilic regions as with oxidized

thiol-terminated monolayers. This approach also affords the opportunity to pattern multiple proteins, unlike amine and carboxylic acid-terminated patterns. In those cases, once one protein is patterned, any coupling to a newly created amine or carboxylic acid region could also result in coupling to the previously immobilized protein.

While photolithographic techniques that are capable of producing submicron DNA³⁸ or biomolecule patterns^{39,40} have been demonstrated, to the best of our knowledge, such methods have not been utilized to fabricate submicron protein patterns. The attainable resolution of photolithography does not match or exceed those of the AFM and stamp-based methods described above. Still, patterning proteins and peptides at the feature sizes achievable by photolithography has value. For example, it has been demonstrated using contact printing and other methods that submicron features formed using fluorescently labeled proteins and peptides can be visualized using standard fluorescence microscopy, making confirmation of binding events facile. Furthermore, patterns of submicron spot sizes are at a biologically relevant length scale for applications in biomaterials and device formation. For instance, submicron protein and peptide assemblies allow for the development of biomaterials that more closely mimic the extracellular matrix (ECM) since integrin receptor clustering and cell binding to the ECM occurs at this scale.^{41–44} The capacity to create protein assemblies in this range is also relevant to developing biohybrid nanodevices.¹ Patterning using photolithography offers certain advantages over the techniques that achieve the same resolution. Batch fabrication using photolithography enables the simultaneous creation of hundreds or thousands of features as well as the ability to sequentially pattern multiple proteins. This increases fabrication rates exponentially with miniaturization of devices, a trend that has fueled the growth of the semiconductor industry. This motivated us to explore submicron protein patterning using photolithography. We anticipated that PDEPMA films could be developed into a platform technology for patterning proteins with a resolution below 1 μm. In this study, we demonstrate for the first time protein patterns at this scale using a photolithographic approach. We also report that protein assemblies are possible within nanowells that are created in the film.

Experimental Section

Pattern Formation. PDEPMA was synthesized as previously described in the literature.³⁶ The spin-coating solution consisted of a 2% w/w solution of PDEPMA in chloroform containing diphenyliodonium-9,10-dimethoxyanthracene-2-sulfonate (DIAS; Aldrich; 5 wt % PAG/polymer). The solution was spin-coated at 3000 rpm with a ramp time of 0.5 s for 30 s on a silicon wafer that had been previously modified by C₄F₈ plasma deposition. C₄F₈ plasma deposition was performed using a Plasma-Therm 770 SLR series system (C₄F₈ flow rate: 100 sccm; argon flow rate: 10 sccm; pressure: 15 mT; inductively coupled plasma power source: 300 W at 13.56 MHz; process time: 10 s; wafer temp: 30 °C). The film was either flood exposed or exposed through a chrome-on-quartz mask for 4 s with a GCA 6300 i-line wafer stepper (UCSB; 180

(20) Li, H. W.; Muir, B. V. O.; Fichet, G.; Huck, W. T. S. *Langmuir* **2003**, *19*, 1963–1965.

(21) Csucs, G.; Kunzler, T.; Feldman, K.; Robin, F.; Spencer, N. D. *Langmuir* **2003**, *19*, 6104–6109.

(22) Hoff, J. D.; Cheng, L. J.; Meyhofer, E.; Guo, L. J.; Hunt, A. J. *Nano Lett.* **2004**, *4*, 853–857.

(23) Falconnet, D.; Pasqui, D.; Park, S.; Eckert, R.; Schift, H.; Gobrecht, J.; Barbucci, R.; Textor, M. *Nano Lett.* **2004**, *4*, 1909–1914.

(24) Kumar, A.; Whitesides, G. M. *Appl. Phys. Lett.* **1993**, *63*, 2002–2004.

(25) Xia, Y. N.; Whitesides, G. M. *Angew. Chem., Int. Ed.* **1998**, *37*, 551–575.

(26) Vossmeier, T.; Jia, S.; Delonno, E.; Diehl, M. R.; Kim, S. H.; Peng, X.; Alivisatos, A. P.; Heath, J. R. *J. Appl. Phys.* **1998**, *84*, 3664–3670.

(27) Nakagawa, M.; Ichimura, K. *Colloids Surf., A* **2002**, *204*, 1–7.

(28) Ryan, D.; Parviz, B. A.; Linder, V.; Semetey, V.; Sia, S. K.; Su, J.; Mrksich, M.; Whitesides, G. M. *Langmuir* **2004**, *20*, 9080–9088.

(29) Hong, L.; Sugimura, H.; Furukawa, T.; Takai, O. *Langmuir* **2003**, *19*, 1966–1969.

(30) Hong, L.; Hayashi, K.; Sugimura, H.; Takai, O.; Nakagiri, N.; Okada, M. *Surf. Coat. Technol.* **2003**, *169*, 211–214.

(31) Lee, K. J.; Pan, F.; Carroll, G. T.; Turro, N. J.; Koberstein, J. T. *Langmuir* **2004**, *20*, 1812–1818.

(32) Aoki, A.; Ghosh, P.; Crooks, R. M. *Langmuir* **1999**, *15*, 7418–7421.

(33) Bhatia, S. K.; Hickman, J. J.; Ligler, F. S. *J. Am. Chem. Soc.* **1992**, *114*, 4432–4433.

(34) Liu, J.; Hlady, V. *Colloids Surf., B* **1996**, *8*, 25–37.

(35) Ichinose, N.; Sugimura, H.; Uchida, T.; Shimo, N.; Masuhara, H. *Chem. Lett.* **1993**, 1961–1964.

(36) Christman, K. L.; Maynard, H. D. *Langmuir* **2005**, *21*, 8389–8393.

(37) Lemieux, G. A.; Bertozzi, C. R. *Trends Biotechnol.* **1998**, *16*, 506–513.

(38) Yin, H. B.; Brown, T.; Wilkinson, J. S.; Eason, R. W.; Melvin, T. *Nucleic Acids Res.* **2004**, *32*, e118.

(39) Poghosian, A.; Platen, J.; Schoening, M. J. *Electrochim. Acta* **2005**, *51*, 838–843.

(40) Platen, J.; Poghosian, A.; Schoening, M. J. *Sensors* **2006**, *6*, 361–369.

(41) Burridge, K.; Fath, K.; Kelly, T.; Nuckolls, G.; Turner, C. *Annu. Rev. Cell Biol.* **1988**, *4*, 487–525.

(42) Burridge, K.; Chrzanowska-Wodnicka, M. *Annu. Rev. Cell Dev. Biol.* **1996**, *12*, 463–518.

(43) Shaw, L. M.; Messier, J. M.; Mercurio, A. M. *J. Cell Biol.* **1990**, *110*, 2167–2174.

(44) Miyamoto, S.; Teramoto, H.; Coso, O. A.; Gutkind, J. S.; Burbelo, P. D.; Akiyama, S. K.; Yamada, K. M. *J. Cell Biol.* **1995**, *131*, 791–805.

mW/cm²) resulting in a dose of 720 mJ/cm². Films that were exposed with a mask were first incubated with an aldehyde reactive probe (ARP; *N*-(aminooxyacetyl)-*N'*-(*D*-biotinoyl) hydrazine; 2 mg/mL; Molecular Probes) for 45 min, followed by Alexa Fluor 568 streptavidin (5 μg/mL; Molecular Probes) for 45 min. To determine if an aminoxy-terminated compound could also be attached to the background of the films, the films were first exposed with a mask, and then incubated with ARP (2 mg/mL) for 45 min. The films were then re-entered into the stepper and flood exposed. They were subsequently incubated with Alexa Fluor 488 hydroxylamine (C₅-aminooxyacetamide, bis(triethylammonium) salt; 100 μg/mL; Molecular Probes) for 45 min, followed by Alexa Fluor 568 streptavidin (5 μg/mL) for 45 min. *O*-(methoxypoly(ethylene glycol))-hydroxylamine ($M_n = 5000$) was synthesized according to a reported procedure⁴⁵ and attached to the background of the films by first exposing newly spin-coated films through a mask, incubating with ARP (2 mg/mL) for 45 min, flood exposing the films, and then finally incubating with the aminoxy-terminated poly(ethylene glycol) (PEG; 1 mg/mL) for 45 min. Immobilization of streptavidin on the original biotin patterns occurred by incubating with Alexa Fluor 568 streptavidin (5 μg/mL) for 45 min. To create protein assemblies, the above procedure was performed, except that unlabeled streptavidin (5 μg/mL; kindly provided by Professor Thomas Ward at the University of Neuchatel) was utilized. Films were then incubated with biotinylated anthrax toxin receptor-1 (ANTXR-1; 200 μg/mL in tris-buffered saline (TBS; pH 7.4)) for 1 h, and then with Alexa Fluor 488 protective antigen (PA; 1.2 μM in TBS containing 1 mM MgCl₂) for 1 h. The K_D of PA-ANTXR-1 interaction *in vitro* is between 130 nM and 1.1 μM, depending on the cations present.⁴⁶ A 1.2 μM concentration was therefore utilized to ensure saturation of the binding sites. All incubation steps were performed by placing a 50 μL drop of solution on the films, covering the samples to prevent dehydration, and finally placing the samples in an incubator at 37 °C. All reagents were diluted in Milli-Q H₂O unless otherwise indicated. Samples were rinsed by first removing the incubation solution, and then placing a 100 μL drop of Milli-Q H₂O for 5 min. This process was repeated three times after each incubation step. After protein patterning and assembly, samples were quickly dried with a stream of air and then immediately analyzed with fluorescence microscopy and AFM. All protein patterns and assemblies were performed in triplicate.

Film and Pattern Analysis. Film thickness was determined with a Rudolph AutoELII ellipsometer (UCSB). Flood-exposed films were incubated with ARP (2 mg/mL) for 45 min and analyzed with X-ray photoelectron spectroscopy (XPS). XPS analysis was performed by the UCSB Materials Research Laboratory on a Kratos Axis Ultra using monochromated Al K α x-radiation. Survey scans were performed at a pass energy of 160 eV with a 0.5 eV channel width, while high-resolution scans were performed at a 20 eV pass energy with a 0.05 eV channel width. Charge compensation was achieved using low-energy electrons from a filament, and peak positions were calibrated by adjusting aliphatic carbon to 284.8 eV. Fluorescence was visualized with a Zeiss Axiovert 200 fluorescent microscope equipped with an AxioCam MRm monochrome camera. Pictures were acquired and processed using AxioVision LE 4.1 and analyzed using Image J 1.33u (NIH). Samples with streptavidin patterns before and after the addition of PEG were prepared at the same time, under identical conditions, and images were acquired using identical microscope and camera conditions. To determine the change in background binding, five areas distributed throughout the background (outside streptavidin patterns) were selected using Image J 1.33u, and the mean pixel intensity for each selection was determined. The average pixel intensities were compared between samples without and with PEG, and the percent reduction in background binding was determined as [(average pixel intensity without PEG - average pixel intensity with PEG)/average pixel

intensity without PEG] \times 100. Immediately after fluorescence analysis, AFM images were acquired with a multimode Nanoscope IIIA system (Digital Instruments) operated in tapping mode using a rotated monolithic silicon probe with a nominal spring constant of 40 N/m and a tip radius less than 10 nm (model BS-Tap300, Nanoscience Instruments, Inc.). Images were acquired as 512 \times 512 pixels with a scan rate of 2.00 Hz. Streptavidin patterns and anthrax toxin receptor/PA assemblies were analyzed sequentially on the same day to minimize changes in humidity. Images were processed and analyzed using a Nanoscope v.5.12r5 (Digital Instruments).

Biotinylation of Soluble ANTXR-1 I Domain. This procedure was adapted from a previously described procedure.⁴⁷ Soluble ANTXR-1 I domain (sANTXR-1) was expressed and purified as previously described⁴⁸ and was incubated at 2 mg/mL with 25 mM dithiothreitol (DTT) at 4 °C for 2 h. Freshly prepared tris-(2-carboxyethyl)phosphine hydrochloride (TCEP) was added to the protein solution at 3 mol of TCEP per mol of sANTXR-1. Reduced sANTXR-1 was added to a 10 mL Sephadex-G25 (Amersham Biosciences) column equilibrated with phosphate-buffered saline (PBS; 2.7 mM KCl, 4.3 mM Na₂HPO₄·7H₂O, 1.4 mM KH₂PO₄, pH 7.4, 137 mM NaCl) and 0.05 mg/mL TCEP, and 1 mL fractions were collected in microcentrifuge tubes containing 15 μL of a 0.5 mg/mL TCEP stock solution. Fractions were visually screened for protein content using BioRad Bradford dye, and those with the highest protein content were combined with a final volume not exceeding 2 mL. O₂ was replaced with N₂ by flowing gaseous N₂ over the protein solution for 5 min. The contents of a No-Weigh Maleimide PEO₂-Biotin Microtube (Pierce) were dissolved in 200 μL of PBS, and 50 μL of this biotin solution was added to the reduced sANTXR-1 sample. The reaction was incubated at room temperature for 2 h. Biotinylated sANTXR-1 was dialyzed overnight in PBS using a Slide-A-Lyzer (Pierce), followed by another 4 h dialysis step. Protein concentration was determined by BioRad Bradford dye, and the biotin incorporation rate was determined by the EZ Biotin Quantitation Kit (Pierce) to be 1.08 mmol of biotin per 1.0 mmol of sANTXR1.

Maleimide Alexa Fluor Labeling of PA. This procedure was adapted from Wiglesworth et al.⁴⁷ A mutant form of PA, in which the glutamate at position 733 is replaced by a single cysteine (E733C), was used to for site-specific labeling. Purified PA(E733C) at 2 mg/mL was incubated with 25 mM DTT at 4 °C for 2 h. Freshly prepared TCEP was added to the protein solution at 1 mol of TCEP per mol of PA. Reduced PA was added to a 10 mL Sephadex-G25 (Amersham Biosciences) column equilibrated with PBS and 0.05 mg/mL TCEP, and 1 mL fractions were collected in microcentrifuge tubes containing 15 μL of a 0.5 mg/mL TCEP stock solution. Fractions were visually screened for protein content using BioRad Bradford dye, and those with the highest protein content were combined with a final volume not exceeding 2 mL. O₂ was replaced with N₂ by flowing gaseous N₂ over the protein solution for 5 min. Alexa Fluor-488 C₅-maleimide (Invitrogen) was added to the PA solution in 10–20 molar excess, and all steps beyond fluorophore addition were light protected. The reaction was incubated at room temperature for 2 h. Alexa Fluor-488-labeled PA was dialyzed overnight in PBS using a Slide-A-Lyzer (Pierce), followed by another 4 h dialysis step. Protein concentration was determined by BioRad Bradford dye and the fluorophore incorporation rate was determined to be 1.3 using the following calculation: (A_x/E) \times (molecular weight of protein/mg protein per mL) = (mol of dye/mol of protein). A_x is the absorbance value of the fluorophore at the absorption maximum wavelength, and E is the molar extinction coefficient of the fluorophore at the absorption maximum wavelength.

Results and Discussion

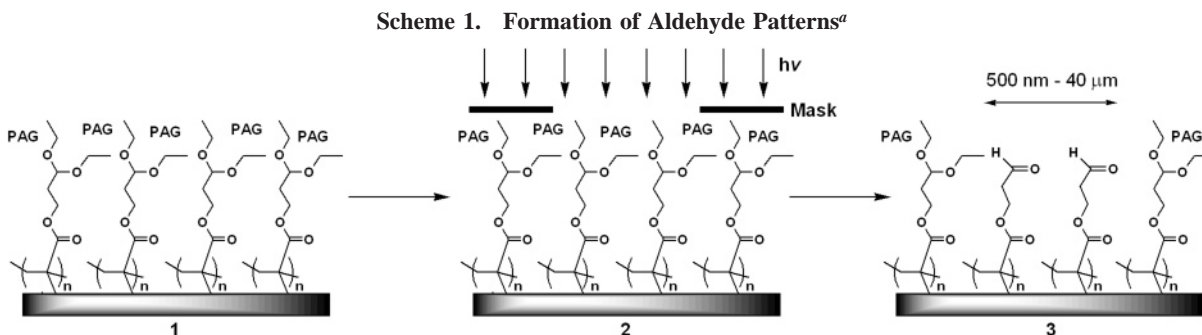
In an effort to simultaneously produce micron and submicron protein patterns, PDEPMA films were exposed

(45) Schlick, T. L.; Ding, Z.; Kovacs, E. W.; Francis, M. B. *J. Am. Chem. Soc.* **2005**, *127*, 3718–3723.

(46) Scobie, H. M.; Thomas, D.; Marlett, J. M.; Destito, G.; Wiglesworth, D. J.; Collier, R. J.; Young, J. A.; Manchester, M. *J. Infect. Dis.* **2005**, *192*, 1047–1051.

(47) Wiglesworth, D. J.; Krantz, B. A.; Christensen, K. A.; Lacy, D. B.; Juris, S. J.; Collier, R. J. *J. Biol. Chem.* **2004**, *279*, 23349–23356.

(48) Bradley, K. A.; Mogridge, J.; Jonah, G.; Rainey, A.; Batty, S.; Young, J. A. *J. Biol. Chem.* **2003**, *278*, 49342–49347.



^a PDEPMA films that include a PAG were formed by spin-coating (1). Following exposure to i-line (365 nm) light through a chrome-on-quartz mask (2), acetals were site-specifically hydrolyzed to aldehydes (3) as a result of localized acid generation.

with a GCA 6300 i-line wafer stepper and a chrome-on-quartz mask. The mask was designed and fabricated to produce features ranging from 500 nm to 40 μm . DIAS, a molecule that is excited at 365 nm light to produce acid, was employed as the PAG. PDEPMA and DIAS were spin-coated onto Si wafers that were first subjected to C_4F_8 plasma treatment. This process rendered the substrate hydrophobic, which promoted better adhesion of the ~ 100 nm thick PDEPMA film. Exposure through the mask resulted in local acid formation, hydrolysis of the acetals, and patterns of aldehyde functionality (Scheme 1).

To develop a platform technology for patterning and producing protein assemblies, we envisioned first creating a micro- and nanopatterned streptavidin foundation. Streptavidin has four binding sites for the high-affinity ligand biotin, and thus can be employed as an adaptor molecule between a biotinylated surface and other biotinylated molecules.⁴⁹ Because there is an abundance of available biotinylated proteins and peptides, the streptavidin platform film could then be tailored for various applications. Therefore, UV-exposed films were first incubated with a biotinylated, aminoxy-containing ARP. Biotin immobilization was confirmed by examining PDEPMA films after flood exposure and incubation with ARP using XPS. XPS scans revealed that original PDEPMA films (Figure 1A, acetal) as well as deprotected films (Figure 1A, aldehyde) contained no nitrogen, whereas the scan of the deprotected films with immobilized biotin (Figure 1A, biotin) displayed a distinct peak at 400 eV (Figure 1A, N arrow), indicating the presence of nitrogen. Peak fitting on the high-resolution nitrogen scan resolved two peaks at 400.8 and 399.7 eV, corresponding to the ureido and the hydrazine, respectively, of ARP (Figure 1B), thus confirming its immobilization on the deprotected films. The oxime nitrogen peak overlaps with the ureido nitrogen peak and is not distinguishable. In addition, there were distinct peaks (Figure 1A, S arrows) at 164 eV (S 2p) and 228 eV (S 2s), which indicates the presence of sulfur, and elemental analysis revealed a 4:1 ratio of N/S, which is close to the 5:1 ratio in ARP. The discrepancy could be due to the fact that the sulfur is in the biotin portion of ARP that should be furthest from the surface, while three of the nitrogens are located in the linker of ARP that attaches to the polymer film and thus should be buried. Background subtraction and the accuracy of sensitivity factors can also affect this ratio.

Following confirmation of biotin attachment, patterned films were then incubated with Alexa Fluor 568 streptavidin. Figure 2A displays the red fluorescent protein within the patterns with minimal nonspecific binding to the acetal background. The mask allowed for feature sizes ranging from 40 μm (largest features in Figure 2) down to 500 nm. Approximately 750 nm spots that corresponded to the original mask patterns were visualized with

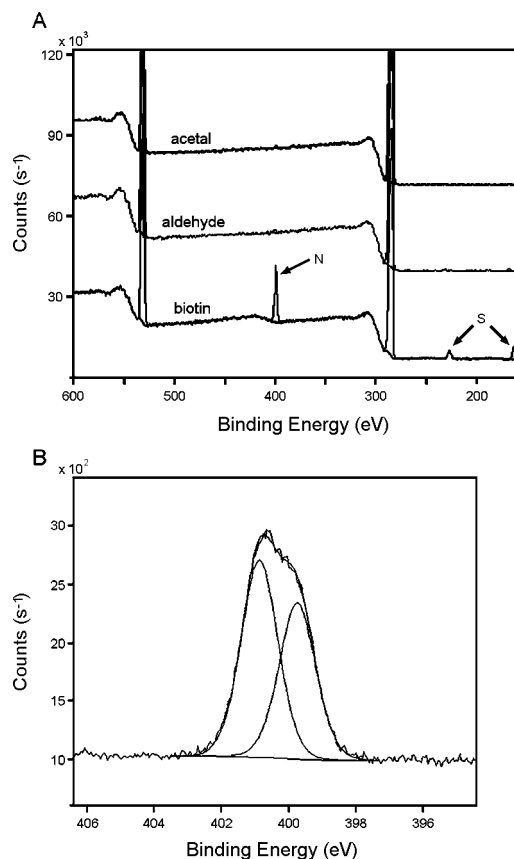


Figure 1. XPS spectra. (A) XPS scans of the PDEPMA film prior to UV exposure (acetal), the film post-deprotection (aldehyde), and the deprotected film post-incubation with a biotinylated ARP (biotin). Only the film with immobilized biotin displayed distinct peaks for nitrogen and sulfur (arrows), confirming the presence of biotin. (B) High-resolution nitrogen scan of film with immobilized ARP (biotin).

fluorescence microscopy, demonstrating that the i-line stepper readily produces submicron resolution feature sizes (Figure 2A, inset). Distinct features below this size were difficult to image. As a control, samples were stained with Alexa Fluor 568 streptavidin without first immobilizing the biotin; as expected, no red fluorescent protein was observed within the patterns or background.

Although minimal nonspecific streptavidin adsorption was observed, it was possible that other proteins would exhibit a higher degree of fouling on the remaining hydrophobic acetal groups. To eliminate this possibility, we envisioned passivating the background with the protein-resistant polymer, PEG.⁵⁰ We anticipated that this could be accomplished by first patterning biotin, then flood exposing the entire film to convert the remaining

(49) Weber, P. C.; Ohlendorf, D. H.; Wendoloski, J. J.; Salemme, F. R. *Science* **1989**, *243*, 85–88.

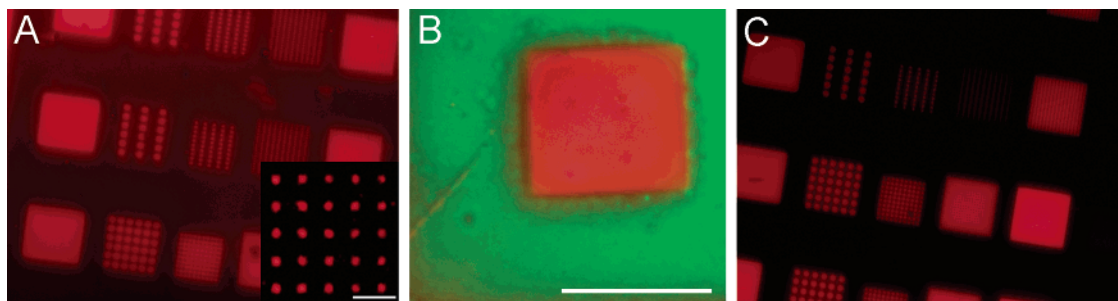
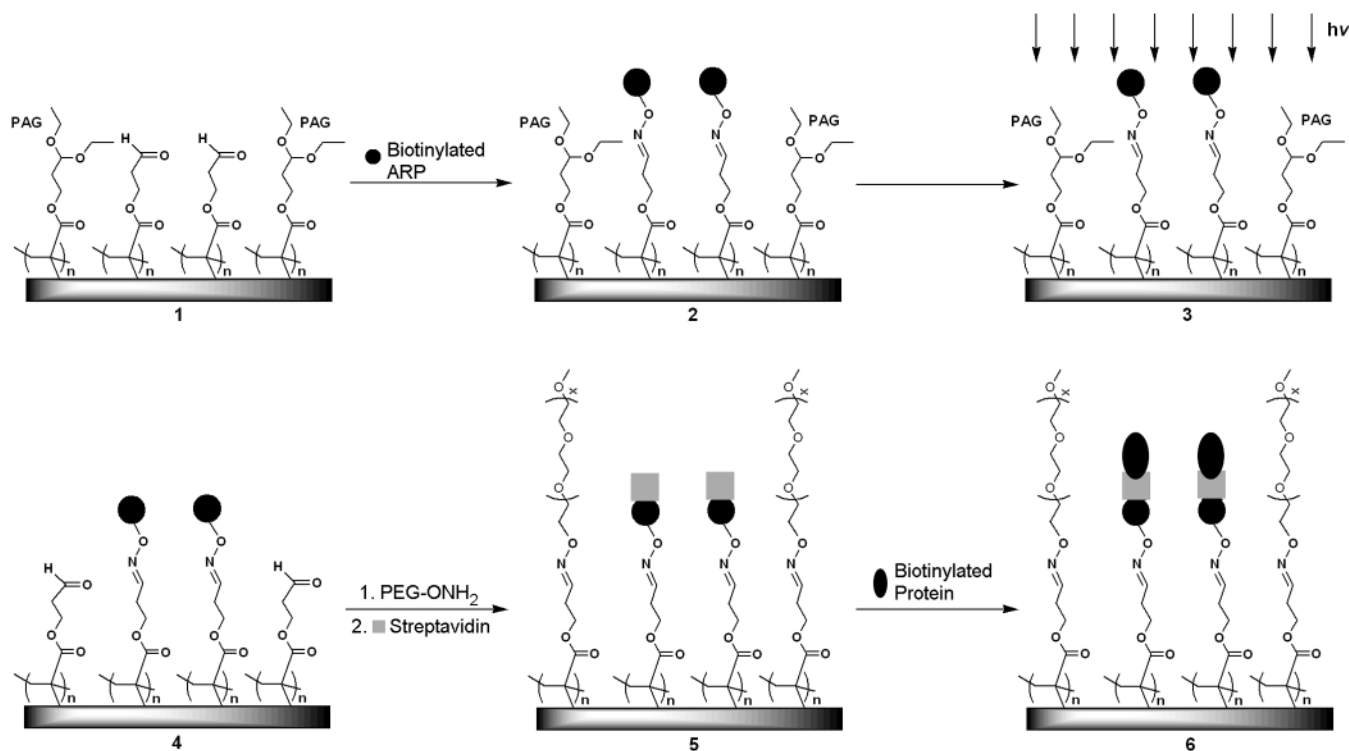


Figure 2. Streptavidin patterns. (A) Streptavidin with acetal background. A PDEPMA plus PAG film was exposed with i-line light through a mask, which contained features sizes ranging from 40 μm to 500 nm, and was then incubated with a biotinylated ARP followed by Alexa Fluor 568 streptavidin. Inset displays submicron streptavidin patterns (scale bar = 5 μm), with the background subtracted for easier visualization. (B) Re-exposed film. Following exposure to 365 nm light through a mask, aminoxy-functionalized biotin was immobilized to newly formed aldehyde groups. Films were then flood exposed with i-line light and incubated with a green fluorescent hydroxylamine, which bound to the hydrolyzed background. Red fluorescent streptavidin then bound to the original biotin patterns. Scale bar = 40 μm . (C) Streptavidin with PEG background. A PDEPMA plus PAG film was initially patterned with i-line light through a mask and then incubated with ARP. The sample was then flood exposed to i-line light and incubated with an aminoxy-terminated PEG, followed by Alexa Fluor 568 streptavidin. Note the reduction in nonspecific protein binding once PEG was added to the background of the films (C vs A).

Scheme 2. Streptavidin Foundation for Protein Patterning and Assembly on a Nonfouling PEG Background^a



^a Following exposure to 365 nm light through a mask, acetal groups were site-specifically converted to aldehydes (1). A biotinylated hydroxylamine (ARP) was attached to converted aldehydes through an oxime bond (2). Films were then flood exposed to i-line light (3), which hydrolyzed the remaining acetals to aldehydes (4). Aminoxy-terminated PEG bound to the background aldehydes, while streptavidin immobilized to biotin patterns (5). Any biotinylated protein can then be immobilized onto the streptavidin foundation (6).

acetals to aldehydes, and finally conjugating an aminoxy-modified PEG (Scheme 2). To confirm that a second exposure would hydrolyze the remaining acetals, the films were first subjected to i-line light through a mask. Following incubation with ARP, samples were flood exposed with the i-line stepper. Films were subsequently incubated with Alexa Fluor 488 hydroxylamine and then Alexa 568 streptavidin. The green fluorescent aminoxy compound bound specifically to the background (Figure 2B), indicating that the second exposure hydrolyzed the remaining acetals. Red fluorescent streptavidin bound to the original pattern, providing evidence that flood

exposure did not affect the immobilized biotin. Given these promising results, an aminoxy-terminated PEG was synthesized. Biotin was patterned, and the film was flood exposed to i-line light. Samples were then incubated with the aminoxy-terminated PEG, followed by the immobilization of red fluorescent streptavidin (Scheme 2, 1–5). The PEG reduced the nonspecific background adsorption of streptavidin (Figure 2C), indicating that the surfaces were rendered protein resistant. Specifically, the average background pixel intensity was reduced to 0.3 with PEG compared to 17.3 without PEG, corresponding to an approximate 98% reduction in nonspecific protein adsorption. After the two exposures, it is likely that the majority of the PAG has been activated; however, it cannot be ruled out that some

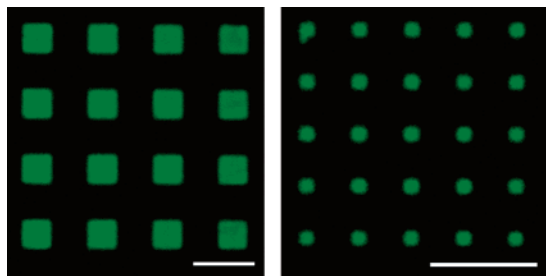


Figure 3. Protein assembly. Samples containing patterned streptavidin with a nonfouling PEG background were incubated with biotinylated ANTXR-1 and green fluorescent PA, resulting in protein assembly at the locations of the original aldehyde patterns. Scale bar = 10 μm .

may still remain trapped within the bottom layers of the polymer film. Nonetheless, samples remained stable for up to two weeks (longest storage time) in air after biotin patterning and flood exposure. Both exposure to ambient light and any possible remaining PAG did not adversely affect subsequent streptavidin or PEG immobilization.

Streptavidin on the surface should contain two available binding sites for biotin; therefore, biotinylated proteins may be assembled onto the streptavidin arrays (Scheme 2, 6). To assess the potential to form protein assemblies on the pH-reactive films, biotinylated ANTXR-1 and the PA component of anthrax toxin were employed as a model system. Anthrax toxin is formed from three proteins secreted by the bacterium *Bacillus anthracis*: edema factor (EF), lethal factor (LF), and PA.⁵¹ PA is the particular moiety that binds to the cellular receptor ANTXR-1⁵²

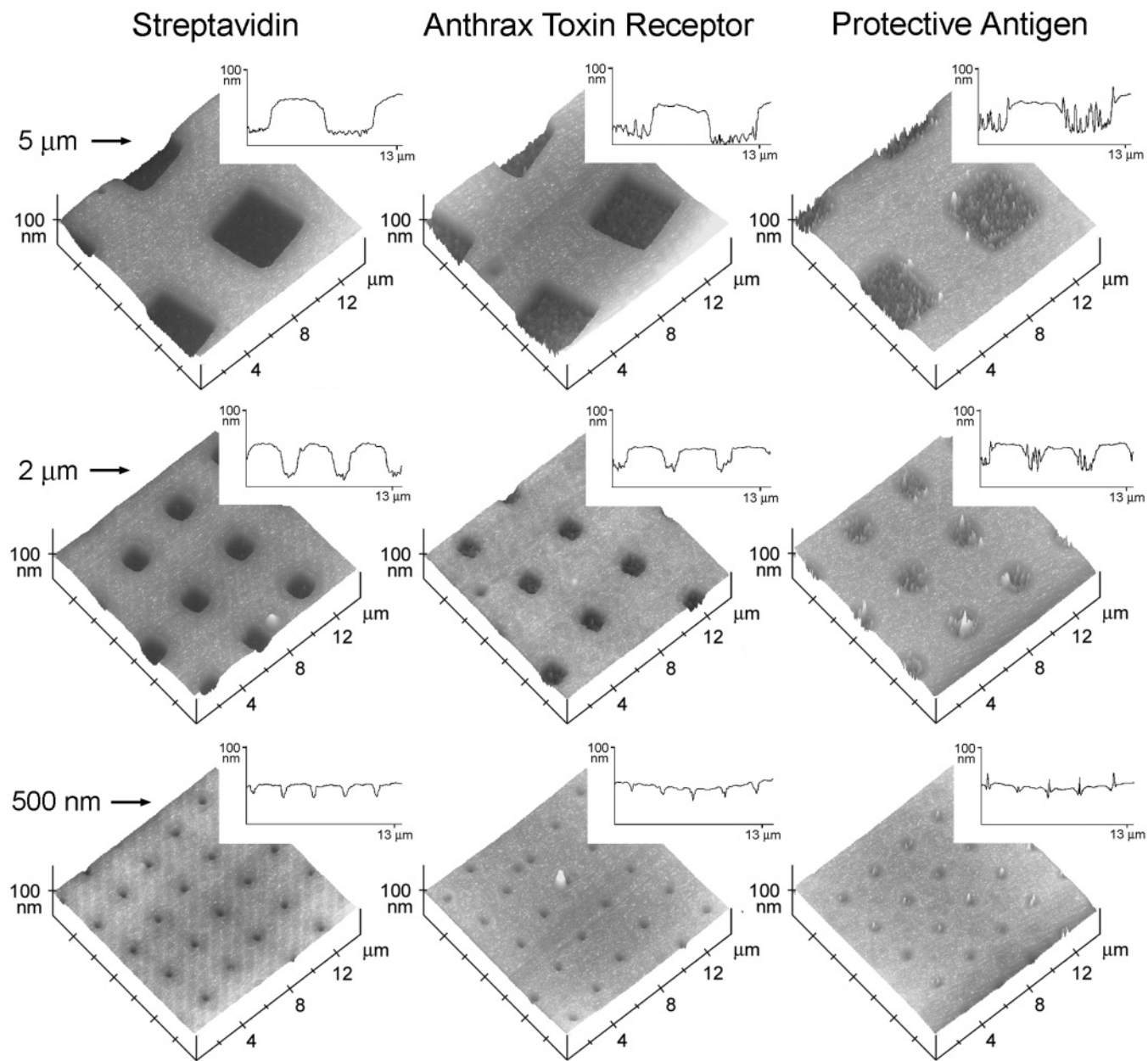


Figure 4. 3D protein assembly. At locations of i-line light exposure, films collapsed upon PAG activation and aldehyde conversion. Streptavidin (left column) was immobilized to patterns with a nonfouling PEG background. Biotinylated ANTXR-1 (middle column) then attached to streptavidin because of its four binding sites for biotin. PA (right column) finally bound to the immobilized ANTXR-1, forming a three-protein assembly on the original aldehyde patterns. Protein patterning and assembly occurred on features sizes as small as 500 nm (bottom row). Graphs on the right are the height profiles through a line of features on the corresponding 3D image.

and allows for the internalization of EF and LF into the cytosol.^{53,54}

Streptavidin patterns with a nonfouling PEG background were fabricated as described above, except that unlabeled streptavidin was utilized. Biotinylated ANT XR-1 was then attached to immobilized streptavidin, and samples were finally incubated with Alexa Fluor 488 modified PA. Green fluorescence was observed only at locations of streptavidin patterns (Figure 3), indicating that protein assembly had occurred with the three proteins on the original aldehyde patterns.

A MultiMode AFM (Digital Instruments) in tapping mode was utilized to further confirm site-specific protein attachment and assembly, as well as visualize features that were below the resolution of fluorescence microscopy. AFM images of the 5 μm patterns revealed that the film collapsed approximately 50 nm at locations of original UV light exposure, creating nanowells for protein immobilization. The collapse is likely due to the release of small molecules upon conversion of acetals to aldehydes and the release of products from PAG activation, followed by polymer chain rearrangement. This collapse is unlikely to be a result of polymer chain degradation due to UV radiation since the collapse was not observed upon exposure in the absence of a PAG. The addition of PEG also contributed to the formation of the wells since the polymer is attached only to the background. Because the polymer substrate and proteins are soft materials, it was difficult to observe a significant height change with the addition of the single protein streptavidin; however, when protein assemblies of biotinylated anthrax toxin receptor and PA were formed, the height change became more distinguishable. Figure 4 displays this protein assembly on three different features sizes: 5 μm , 2 μm , and 500 nm. Changes in height upon protein assembly were measured in the 5 μm features since binding occurred mainly at the bottom of these wells. An average height change of 8 ± 2 nm was detected upon binding of the ANT XR-1 within the nanowells that had an original depth of ~ 50 nm. An increase of 11 ± 3 nm was then observed following the addition of PA. As demonstrated in Figure 4, the height of the protein assemblies on the film was not uniform, which is likely due to the characteristics of the proteins. Biotinylation of ANT XR-1 occurred on two possible amino acids. Thus, the biotinylated ANT XR-1 could bind to streptavidin in two different orientations, resulting in height variations for the protein assemblies. Furthermore, the structure of PA is rodlike ($100 \times \sim 50 \times 30$ Å) rather than spherical,⁵⁵ which would also allow for varied height profiles. Nonetheless, the apparent height change corroborates the fluorescent data and further indicates that protein

assemblies are formed. Immobilization and assembly of proteins was observed by AFM in nanowells with a width of 500 nm. This demonstrates the ability to form protein assemblies with a resolution below 1 μm using the pH-reactive polymer PDEPMA. As a control, samples were stained as described above, minus the streptavidin incubation. Samples were also stained with nonbiotinylated ANT XR-1. Green fluorescent PA was not observed with either control. Moreover, no protein assemblies were detected with AFM. This provides further evidence that protein assembly on PDEPMA films occurs via specific biotin–streptavidin interactions.

Conclusions

We demonstrated nanowells with aldehyde functionality for patterning and assembling proteins. Aldehyde patterns are first generated by exposing pH-responsive films containing PDEPMA and a PAG to i-line light through a mask, allowing for the conjugation of aminoxy-modified biotin and the immobilization of streptavidin. Using this technique, protein patterns within nanowells with a width as small as 500 nm were realized. Current semiconductor processing technologies allow even smaller features to be fabricated by photolithography. Taking measures to enhance resolution, this technique can further miniaturize features. The assembly of ANT XR-1 and PA was used as a model system to demonstrate that protein assembly within the wells is achievable. There exists a multitude of biotinylated proteins and peptides, thus this system could be adapted for any number of applications. For example, stacking proteins at the submicron and nanometer length scale is of interest for nanomanufacturing, where one could use the streptavidin patterns as a platform for the fabrication of two- and three-dimensional (3D) constructs. Because of the ease and speed of photolithography, this system would also allow for the facile patterning of multiple proteins and peptides at the necessary resolution for many biomaterial applications, thus adding to the existing arsenal of patterning techniques. For example, integrin clustering, which is required for a full cellular response and attachment to the ECM, is on the order of a few hundred nanometers to micrometers.^{41–44} Therefore, developing biomaterials with patterned ECM proteins, fragments, or peptides could also be achieved with the platform developed in this study. In conclusion, this methodology provides a general strategy for protein immobilization and assembly for various applications in medicine and biotechnology.

Acknowledgment. This work was supported by the NSF (K.L.C., V.D.E.-R., H.D.M.) through SINAM (DMI-0327077) and NIH Grant AI-057870 (S.C.W. and K.A.B.). CNSI and Hewlett-Packard (H.D.M.) are also thanked for providing funding, and the NIH NHLBI is acknowledged for an NRSA postdoctoral fellowship (K.L.C.).

LA0608213

(51) Bradley, K. A.; Young, J. A. *Biochem. Pharmacol.* **2003**, *65*, 309–314.

(52) Bradley, K. A.; Mogridge, J.; Mourez, M.; Collier, R. J.; Young, J. A. *Nature* **2001**, *414*, 225–229.

(53) Friedlander, A. M. *J. Biol. Chem.* **1986**, *261*, 7123–7126.

(54) Milne, J. C.; Collier, R. J. *Mol. Microbiol.* **1993**, *10*, 647–653.

(55) Petosa, C.; Collier, R. J.; Klimpel, K. R.; Leppla, S. H.; Liddington, R. C. *Nature* **1997**, *385*, 833–838.